The association of transequatorial loops in the solar corona with coronal mass ejection onset

A. Glover, L. K. Harra, S. A. Matthews, and C. A. Foley

Mullard Space Science Laboratory, Holmbury St Mary, Dorking, Surrey, RH5 6NT, UK

Abstract. It has been shown that transequatorial loops can disappear in association with the onset of a coronal mass ejection (CME) (Khan & Hudson 2000). We extend this result by considering a larger sample of transequatorial loop systems (TLS) to investigate their associated flaring and CME activity. We find 10 of a total 18 TLS considered here to be associated with flaring and CME onset originating from a connected active region. A total 33 cases of flaring and associated CME onset are observed from these 10 systems during their lifetime. We observe the influence of this activity on the TLS in each case. In contrast to the Khan & Hudson result, we find evidence that transequatorial loop eruption leading to soft X-ray brightening equivalent in temperature to a B-class flare is equally as common as dimming in the corona. Consequently we conclude that the scenario observed by Khan & Hudson is not universal and that other types of CME-TLS association occur. It was found that for transequatorial loops that were associated with CMEs the asymmetry in longitude was larger than for those that were not associated to a CME by 10°. In addition, the extent in latitude (as a measure of the loop length) was nearly twice as large for those TLS associated with CMEs than those that were not. The asymmetry in latitude was actually on average larger for those TLS not associated with CMEs, than for those that were. This suggests that differential rotation is not a major contributor to the production of CMEs from transequatorial loops. Instead it is more likely for a CME to be produced if the loop is long, and if there is a large asymmetry in longitude. The implications of these results for CME onset prediction are discussed.

Key words. coronal mass ejections (CMEs), flares

1. Introduction

The first direct observations of transequatorial interconnecting loops were made by Chase et al. (1976) using data from the Skylab soft X-ray imager. These authors identified 100 loops connecting 94 separate active regions. Loops were found to have an average length of 20° with a maximum 37° separation in heliographic latitude. More recent results (Pevtsov 2000; Farnik et al. 1999) have shown that this observed maximum was biased to lower values owing to the relatively short 9 month period of Skylab's operation, close to the minimum of solar cycle 21. During this period the average active region latitudes were confined within a narrow range. Pevtsov (2000) studied interconnecting loops observed by the Yohkoh soft X-ray telescope (Tsuneta et al. 1991) during the period 1991 to 1998. This study incorporated observations made during the declining phase of solar cycle 22 through to the rising phase of cycle 23, thus removing any bias arising from the variation in active region latitude separation over the course of a solar cycle. This study found the average footpoint separation of transequatorial loops connecting regions in either hemisphere to be approximately 30° with a maximum of 75°. To date no observations of loops connecting regions in the same hemisphere with length

greater then 30–35° have been made. This led Farnik et al. (1999) to propose that an additional process must act on transequatorial loops, in order to account for their increased length. This process would need to have little influence on loops confined to one hemisphere. As such, differential rotation was initially proposed as this additional mechanism. Further study by Pevtsov (2000) however, found 85% of active region pairs connected by transequatorial loop systems to rotate at similar rates in either hemisphere and thus he proposed that differential rotation would have a minimal effect on the evolution of the connected loop system.

The origin of these long transequatorial loops is thought to be reconnection in the corona. Current models assume that active region flux is most likely to emerge from the photosphere independently in each hemisphere (e.g. Moreno-Insertis 1986). Thus, transequatorial loops should form via reconnection in the corona. Tsuneta (1996) presented observations of a transequatorial loop system which appeared to show an X-type neutral point in projection near disk centre. In this study, Tsuneta also noted the appearance of "remarkable flare-like cusp structures" which formed as the region rotated towards the west limb. These were interpreted as evidence that the connection between two active regions constituted a larger "active area" within which reconnection could take place with less explosive consequences than normally observed in active regions.

A number of studies (e.g. Pevtsov 2000; Svestka & Howard 1981) have observed cases where a connection existed between an active region and a region of quiet Sun in opposite hemispheres prior to the emergence of an active region in the connected quiet Sun area. This is suggestive of reconnection taking place as the new active region flux emerges. Pevtsov found only one case where a transequatorial connection was observed to form between two mature active regions. In 40 of a total of 87 cases studied by Pevtsov, a mature active region was observed to be connected to a region of quiet Sun, with a second active region often appearing later in the previously connected quiet Sun area.

Several studies have been undertaken with the intention of gaining insight into the origin and formation of transequatorial loops. However, these structures have only recently been associated with the onset of coronal mass ejections (CMEs) (Khan & Hudson 2000). These authors observed a series of homologous disappearances of an interconnecting loop system. Each disappearance was observed to take place in association with a flare of M-class or above from one of the two connected active regions and CME onset. The results of Khan & Hudson are important in the context of CME onset studies owing to the observed disappearance of approximately 10^{15} g of coronal material from the transequatorial loop systems seen in Yohkoh Soft X-ray Telescope (SXT) images. This is close to the currently accepted mass value for CMEs and may, therefore, account for CME ejecta later observed in coronagraph data. Harrison (1986) illustrated that CME onset may take place in association with a flare located at an asymmetrical position relative to the CME axis. Following this observation, this class of CME onset shows associated flaring to take place within an active region located at one end of the disappearing loop system, prior to disappearance. CMEs are large-scale structures and the disappearance of transequatorial loops in this manner has provided evidence for a related large scale structure leaving the Sun's atmosphere.

This paper extends the findings of Khan & Hudson (2000), who analysed a single eruptive system of loops, to consider a total of 18 interconnecting loop systems in order to investigate how often they are linked to CMEs and flares, how the transequatorial loops respond to flaring and CMEs and the possible influence of differential rotation. In total we observed 33 events associated with 10 of these 18 TLS. The remaining 8 transequatorial loop systems (TLS) were not associated with significant CME activity during their lifetime. The implications of these results in terms of CME onset prediction will be discussed.

2. Observations

For the purposes of this study, we have considered full disk Yohkoh Soft X-ray Telescope (SXT) observations of 18 transequatorial loop systems (TLS) having a resolution of 4.9″ and 9.8″ per pixel. SXT (Tsuneta et al. 1991) uses a grazing incidence telescope and filters which image soft X-rays in the energy range 0.25–4.0 keV. These data were used to identify the TLS and study their morphology. Images taken using the Al.1 and AlMg filters were primarily studied. These are the thinnest of the available SXT filters, and thus provide the clearest observations of faint transequatorial loop systems.

In 16 cases out of 18, TLS were taken from the list published by Pevtsov (2000). The Pevtsov list consists of 87 loop systems. However, for the purposes of this study it was necessary to produce a comparison between SXT observations and data from the suite of instruments onboard SOHO (Solar and Heliospheric Observatory) (Domingo et al. 1995) in order to determine the existence of CMEs. Consequently, only TLS observed after January 1996 could be incorporated. A further two cases were neglected as they appeared very faint in SXT data. This reduced the number of applicable examples from the Pevtsov list from 87 to 16, to which two further TLS, not previously included in the Pevtsov study, were added.

In order to determine whether any TLS was associated with a CME, comparison was made between CME observations (from the SOHO Large Angle Spectroscopic COronagraph (LASCO) (Brueckner et al. 1995)) and changes in the TLS morphology observed throughout the period during which the loop system was visible on the disk. In numerous cases, TLS brightening was observed in association with activity from one or both of the connected active regions.

Determination of the CME onset site and the TLS morphology were also studied by analysing EUV data from the SOHO Extreme Ultraviolet Imaging Telescope (EIT) (Delaboudiniere et al. 1995). EIT Fe XII (195Å) data were available at two resolutions: 2.6″ and 5.2″ per pixel. EUV morphology changes were observed using a "percentage difference" technique: consecutive images were subtracted from each other and divided by the earlier image, as described by Thompson et al. (1998). In the event that a CME was observed in LASCO coronagraph data, CME onset time and location were estimated through comparison with observed disk activity. CMEs were disregarded if an origin other than that of the TLS or connected active regions under investigation could be determined from disk observations. The origin of the CME was investigated by searching for any of the signatures listed below;

(i) EUV dimming, for example, in the vicinity of active regions or the TLS;
(ii) coronal waves or propagation of material;
(iii) flaring;
(iv) changes in the brightness of the TLS;
(v) prominence eruption or;
(vi) the formation of a cusp feature.

These features have been described many times in the literature (e.g. Hudson & Cliver 2001) as having associations with CMEs and allow us to estimate the position of the CME launch site. If one or more of these features were seen close to the estimated CME onset time derived from LASCO height-time extrapolation, then we were confident of the CME origin.

The study by Khan & Hudson (2000) illustrated a series of disappearances in soft X-ray data of a single transequatorial loop system. Each of these disappearances was observed to be similar in appearance, termed "homologous" by the authors, and each took place in association with CME onset. Together with theoretical implications from the Babcock model of the solar cycle, this has led to the suggestion that transequatorial
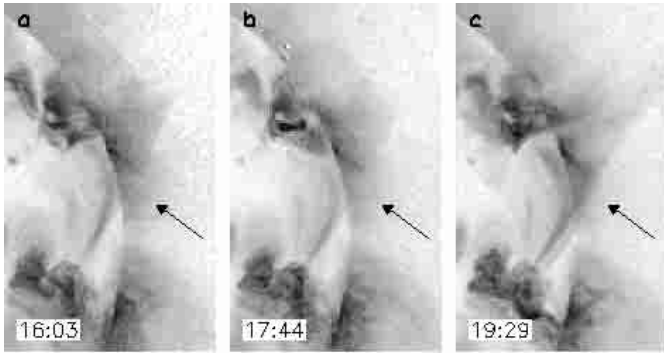
Fig. 1. A TLS that developed into a bright cusp on 12th Mar. 2000 as a response to a CME. Images are taken using the SXT AlMg filter at resolution 4.9″ per pixel. The field of view (FOV) of the images are 15.6′ by 22.1′. **a)** shows the pre-flare TLS, **b)** illustrates the brightening of the northern active region **c)** shows the cusp shaped feature observed following CME onset. This event is in category A.

Fig. 2. SOHO/EIT 195Å percentage difference images (20%) illustrating the event onset on 12th March 2000 from the northern hemisphere active region. This is an event from the "A" category which shows a response in the TLS to the CME. The FOV of the images are 15.6′ by 22.1′. A bright region showing material moving away from the northern active region is observed in **b)** together with a brightening in the vicinity of the active region. **c)** illustrates dimming in the vicinity of the northern active region when compared to the pre-event image **a)**. Images are 5.2″ per pixel resolution.

loop systems (TLS) can have a high probability of eruption. Of the 18 cases considered, during this study however, 8 showed no link with CME activity, either associated with the interconnecting loop system itself or the connected active region(s). The remaining systems did prove to be associated with CME onset and had flaring activity originating in an active region to which the TLS was connected.

We searched for evidence of clear eruptive signatures of the loop system itself, following CMEs during the lifetime of the TLS. An example of the formation of a cusp is shown in Fig. 1. A bright cusp can be interpreted as providing evidence of eruption and magnetic reconnection (e.g. Tsuneta 1992). We determined the temperature of the cusp that formed on the 12th March 2000 observed by SXT using the standard filter ratio technique (Al.1 and AlMg filters). We found that the TLS reached an average temperature of 5.5 MK following the CME. Tsuneta (1996) found that the temperature of the TLS that he studied reached 7 MK. The average temperature value for the diffuse background corona in streamers has been determined by Foley et al. (2002) and was found to be 1.4 MK at solar minimum and 2.2 MK at solar maximum. Consequently the 12th March 2000 TLS has a temperature that is significantly above this level and that can be compared to flare temperatures. The statistical study of Feldman et al. (1995) found that a temperature of around 5.5 MK would be equivalent to that of a low GOES B class flare. A further example of TLS brightening in association with a CME is shown in Fig. 4.

The 18 TLS analysed over the course of this study were separated into 2 categories as follows:

(A) the TLS and/or a connected active region was associated with CME activity and
(B) neither the TLS nor any connected active region was associated with CME activity.

Table 1 lists the 33 eruptive events observed to originate with flaring in one or more of the active regions associated with the 10 TLS systems in Category A and Table 2 lists those TLS unconnected with significant CME activity. The number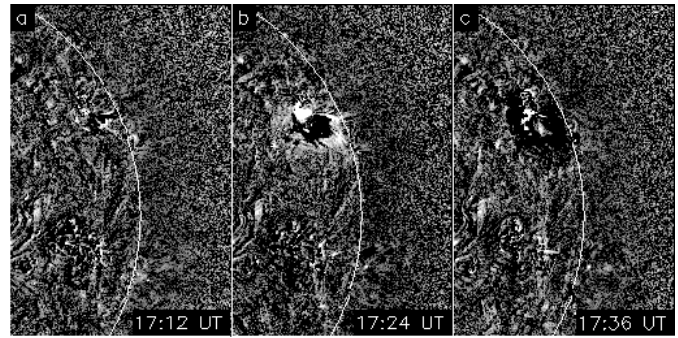 of connected active regions ranges between 0 and 2 and indicates whether the ends of the TLS appear consistent with the location of active regions on the disk. In addition, TLS morphology changes are recorded in the category "eruptive signature" for Category A. The northern and southern location of the ends of the TLS are indicated in terms of whether the TLS appears to end in an active region or in the quiet Sun.

3. Results

Table 1 lists Category A TLS. There are 10 cases listed in this table showing evidence of the TLS itself being involved in eruption leading to enhancement in soft X-ray images, with 2 of these developing into a cusp. This is in contrast to the disappearances observed by Khan & Hudson (2000), although we note that both cases of cusp formation were followed by substantial dimming in the region of the TLS. In each case, EIT 195 Å observations of the interconnecting loop system located near to the west limb illustrate activity originating with flaring from one of the two connected active regions.

3.1. The formation of Brightened features in TLS

Figure 2 illustrates flaring of the northern active region observed in EIT Fe XII (195 Å) for the 12th March 2000 event. Images are percentage difference and show regions undergoing a change in brightness of between ±20%. This sequence of images shows the event initiation occurring between 17:00 and 17:12 UT, where material movement can be seen close to the northern connected active region. The appearance of this motion is similar to that shown in coronal waves (e.g. Thompson et al. 1999). However, if this feature is a coronal wave it is not a long-lasting event and does not travel a large distance across the disk. The observed motion in EIT data corresponds to movement in the SXR TLS close to the northern active region during the same period. This is indicated in Fig. 1b.

The northern active region flare is followed by another flare of magnitude C6.4 from the southern connected active region.

Table 1. CME Activity associated with Category A TLS. Dates on which CME activity associated with the TLS was observed, number of active regions connected by the TLS and the eruptive signature of the TLS itself when involved in eruption are listed.

CME Activity	Connected ARs	Eruptive Signature	North Location	South Location
10-Sep.-97	2	dimming	N22E13	S25E40
21-Oct.-97	1/QS	formation	N20E00	S09W02
02-May-98[a]	2	dimming/disappearance	N26E33	S17W10
04-May-98	2	dimming	N27E06	S17W36
04-May-98	2	none	N27E06	S17W36
06-May-98[a]	2	disappearance	N27W23	S17W60
06-May-98[a]	2	none	N27W23	S17W60
06-May-98[a]	2	none	N27W23	S17W60
07-May-98[a]	2	none	N27W34	S15W75
07-May-98[a]	2	none	N27W34	S15W75
08-May-98[a]	2	disappearance	N28W48	behind limb
08-May-98[a]	2	brightening	N28W48	behind limb
08-May-98[a]	2	dimming	N28W48	behind limb
08-May-98[a]	2	none	N28W48	behind limb
09-May-98[a]	2	disappearance	N28W61	behind limb
09-May-98[a]	2	none	N28W61	behind limb
09-May-98[a]	2	brightening	N28W61	behind limb
27-May-98[b]	2	dimming	N18W52	S24W89
27-May-98[b]	2	brightening	N18W52	S24W89
28-May-98[b]	2	brightening	N18W66	S24W90
29-May-98[b]	2	brightening	N18W81	behind limb
29-May-98[b]	2	dimming	N18W81	behind limb
29-May-98[b]	2	none	N18W81	behind limb
29-May-98	2	disappearance	N26E21	S22W13
15-Oct.-98	2	dimming	N15W12	S21W29
04-Nov.-98	2	None	N18E07	S25W05
24-Nov.-98	2	brightening	behind limb	S18E71
24-Nov.-98	2	none	behind limb	S18E71
25-Nov.-98	2	cusp + dimming	N17E77	S19E68
25-Nov.-98	2	disappearance	N17E77	S19E68
5-Dec.-98	2	None	N16E26	S16W06
12-Mar.-00[b]	2	brightening	N24W45	S13W45
12-Mar.-00[b]	2	cusp + dimming	N24W45	S13W45

[a] indicates that the TLS is also the system studied by Khan & Hudson.
[b] indicates TLS not part of initial Pevtsov (2000) study.

This flare peaks at 18:51UT. A CME is observed in the north west quadrant of LASCO/C2 37 min later. Figure 1 illustrates Yohkoh/SXT data for this period. The soft X-ray loops undergo brightening and morphology change to form a cusp shaped feature that is initially observed at 19:03 UT and illustrated in Fig. 1c. Dimming was also observed in the region of the TLS following cusp formation. LASCO/C2 data for the same period, shown in Fig. 3, illustrates the propagation of a loop-like CME through the north west quadrant of the coronagraph. The accompanying TLS light curve shows gradual brightening of the cusp shaped feature and a peak coinciding with the C6.4 flare onset. The TLS is observed to fade following flaring and CME onset. A second CME from this loop system also showed brightening, but no cusp formation in this instance.

Figure 4 illustrates the changing intensity of another TLS observed using Yohkoh/SXT. These images show the first event listed in Table 1 as having taken place on 29th May 1998. A diffuse collection of interconnecting loops illustrated in Fig. 4a is observed to brighten in association with CME onset (Figs. 4b and c). Following activity from the northern connected active region, these loops take on a cusp-like appearance in projection, situated above the west limb. This is illustrated in Fig. 4c. Unfortunately, the full extent of the loop exceeds the SXT field of view and so this brightening cannot be classified as a cusp. Other CMEs related to this system showed a variety of responses, including either dimming or else no response at all. Hence even within one TLS, one consistent response to CME onset cannot be guaranteed.

EIT 195Å observations for the same period as that illustrated in Fig. 4 show dimming taking place above the west limb confined within the latitudinal extent of the TLS. Following this dimming, the EUV counterpart of the TLS shows a change in
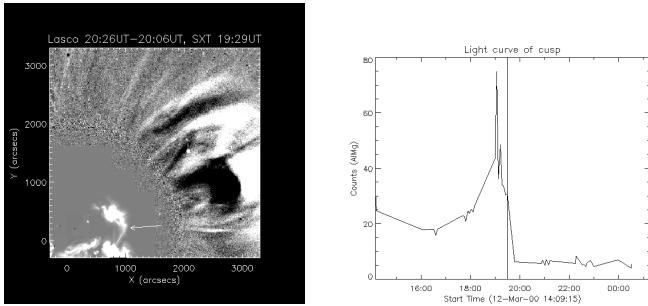
Fig. 3. The figure on the left shows LASCO/C2 difference image (20:26 UT–20:06 UT) illustrating a loop-like CME associated with the soft X-ray brightening of TLS on the 12th March 2000. The SXT AlMg image at 19:29 UT is overlaid, showing that the direction of propagation of the CME is consistent with the location of the north active region, and the TLS. An arrow highlights the position of the cusp in SXR (see Fig. 1). The figure on the right shows the light curve of the cusp illustrating how the feature brightens and then dims in relation to the CME. The CME appears in LASCO C2 at 19:28 UT, and this is illustrated by a vertical solid line.
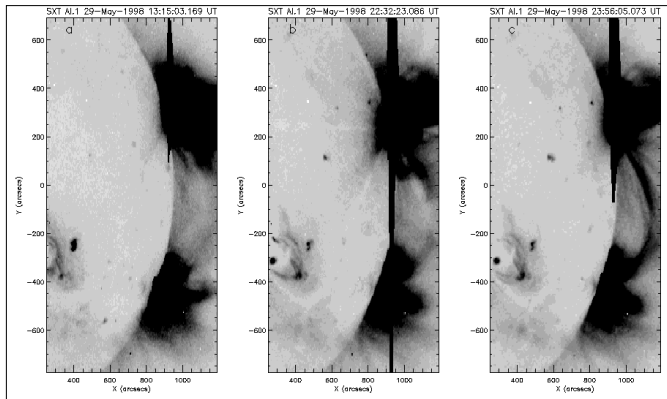
Table 2. Category B lists TLS with active regions and TLS being unrelated to any significant coronal mass ejections. "1/CH" denotes TLS is anchored between an active region and a coronal hole boundary. "QS only" indicates TLS is anchored to regions of quiet sun at either end. Dates are in accordance with Pevtsov (2000).

Clearest Observation	Connected Active Regions	Northern Location	Southern Location
2-Feb.-96	QS	N20W07	S01W06
18-Dec.-96	2	N18W15	S00W01
31-Jan.-97	1	N03E20	S00W28
23-May-97	1	N02W13	S10W46
28-Dec.-97	2	N20E41	S22E01
13-May-98	1	N25W01	S20W05
16-Jun.-98	QS	N32E10	S17W08
15-Nov.-98	1/CH	N20W07	S01W06

Fig. 4. SXT Al.1 images having 4.9″ per pixel resolution showing soft X-ray brightening associated with C3.1 GOES event and CME onset on 29th May 1998 (from category A). **a)** shows that a faint connection existed between the two active regions in soft X-ray data prior to the event. **b)**, taken during the flare, shows an increase in X-ray intensity between the active regions together with some saturation in the vicinity of the flaring active region. **c)** illustrates the brightening of what appears to be an interconnecting cusp shaped feature although the full extent of this feature is beyond the field of view.
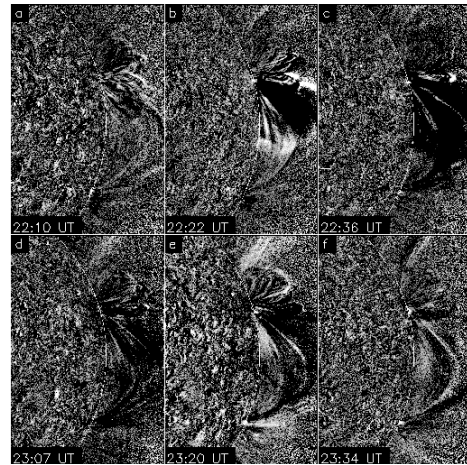

Fig. 5. Coronal EUV dimming observed in association with TLS A2 on 29th May 1998. Images are percentage difference (20%), illustrating morphology changes observed in EIT 195 Å data at a resolution of 2.6″ per pixel. The FOV of each image is 15.8′ × 22′. **b)** illustrates evacuation of material from the vicinity of the northern active region. This dimming is seen to extend **c)** to the width of the transequatorial loop system. Off limb brightening to the north of the dimming region (**b)**, **c)**, **d)**) takes place as nearby coronal streamers are displaced by the eruption. Bright loops begin to appear in the dimming region (**e)**, **f)**) following eruption and prior to the first observation of the cusp shaped feature in SXT (Fig. 4).

loop morphology. Figures 5e and f illustrate the brightening of the loop system between 23:07 and 23:20UT. This system is faint prior to eruption and is spatially consistent with the bright loops seen in soft X-ray data (Fig. 4c).

Comparison of Figs. 4 and 5 with LASCO/C2 and C3 data shows CME onset of the streamer blowout class (Howard et al. 1985). An initial streamer enhancement was observed in the C2 field of view at 22:30 UT on 29th May. This extended out slowly into the corona, without a clear front. Following this, and initially observed in C2 at 00:28 UT on the following day (30th May), a plasmoid is ejected along the same latitude. This two part structure, illustrated in Fig. 6 is frequently observed as a result of streamer disruption (Andrews & Howard 1999; Sheeley et al. 1982).

Comparison with EUV dimming observed in Fig. 5 shows that the plasmoid ejection occurs after the initial dimming onset. The first observation of the streamer enhancement at 22:30 UT in LASCO/C2 is closely related in time to both this initial dimming and brightening observed in SXT data at 22:28 UT (Fig. 4b).

3.2. Disappearance and dimming of the TLS

Table 1 lists 6 cases where a TLS undergoes disappearance in association with CME onset. Of these 6 events, 3 are from the region studied in detail by Khan & Hudson (2000). This system undergoes a series of 3 homologous disappearances of the interconnecting loops. A further disappearance (or dimming) of
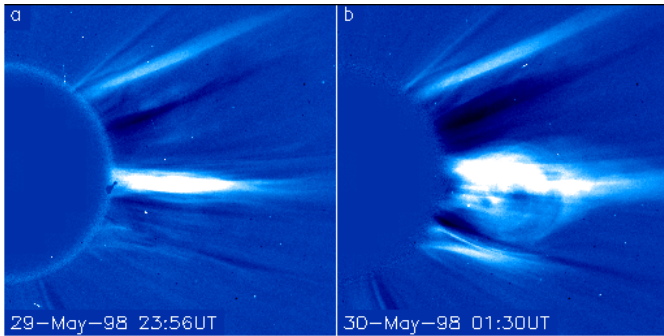
Fig. 6. LASCO/C2 data illustrating the propagation of a streamer blowout CME observed in association with the soft X-ray brightening of TLS-A2 on 29th May 1998. **a)** shows streamer brightening at 23:56 UT. This is followed at 00:28 UT by a plasmoid ejection extending along approximately the same angle. **b)** illustrates the appearance of this plasmoid at 01:30 UT.

this system in connection with CME onset was identified by Wang et al. (2002) on 2nd May 1998. However, Yohkoh spacecraft night meant that it was not possible to determine whether a sudden disappearance or gradual dimming of the TLS took place in this case.

In these cases, eruption leads to a dimming in soft X-ray emission observed in association with flaring and CME onset as opposed to the brightened structures that we also observe in TLS eruptions. Of the 33 CME onset events considered for the purposes of this study, 14 show either a disappearance of the type observed by Khan & Hudson or a slow dimming following a CME. Of these 14 two cases first show cusp formation prior to the dimming onset. Figures 7b and c illustrate a TLS that remained intact following CME onset but faded gradually over a period of several hours.

3.3. Gradual brightening and dimming of a TLS

Figure 7 provides an example of soft X-ray brightening observed in one TLS. In this case, 2 CMEs are observed to originate from the northern active region. Neither CME appears to have a direct effect on the TLS morphology; the TLS appears unchanged in SXT data directly following flaring and the estimated CME onset time. Instead, a gradual brightening of the soft X-ray loops is observed over a period of hours following the first CME onset (Fig. 7b) and a gradual dimming is observed over several hours following the second CME (Fig. 7c). This dimming differs from the type observed by Khan & Hudson as no sudden decrease in emission is observed. In this case, the TLS remains intact following CME onset, fading gradually over a period of hours during which flare activity continues from the two connected active regions.

3.4. The appearance of a TLS

The 21st October 1997 event showed no transequatorial connection in Yohkoh/SXT data prior to CME onset. In this case, previously unobserved loops were seen following CME onset and flaring from the northern active region. These
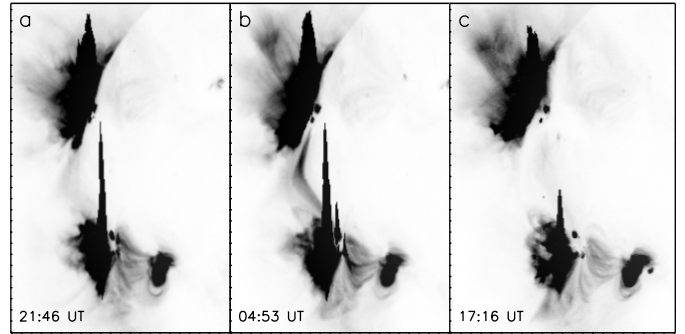

Fig. 7. SXT data having 4.9″ per pixel resolution illustrating morphology changes associated with CME onset on 25th November 1998. Two CMEs are observed on 24th November. In both cases the TLS remains unchanged after CME onset. This figure illustrates gradual changes in TLS brightness observed over the surrounding period of the CMEs observed on 25th November covering 20 hours from 21:46 on the 24th. The FOV of the images is 18′ × 24′. Brightening is observed **b)** following the first onset at 04:40 UT while a gradual dimming **c)** of the TLS occurs following the second onset at 12:15 UT.
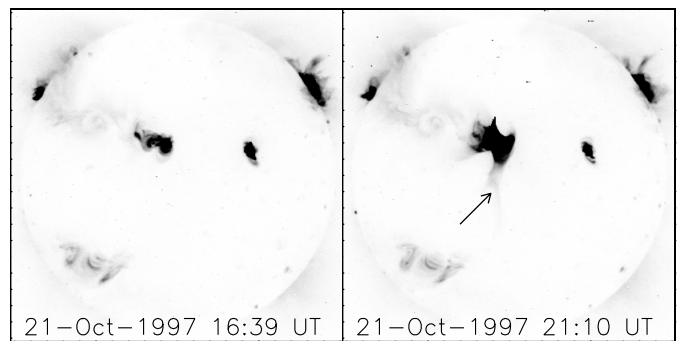

Fig. 8. Yohkoh/SXT data illustrating the appearance of a transequatorial connection in soft X-ray data following flaring and CME onset in the sigmoidal active region AR 8097 on 21st October 1997. The TLS is indicated by an arrow in **b)**. These loops are seen to fade gradually over a period of several hours. SXT data has resolution 4.″9 per pixel. Solar north points up and east to the left.

loops stretched across the equator, as illustrated in Fig. 8. Comparison with EIT 195 Å data shows no comparable EUV dimming in this case. Consequently, the bright soft X-ray loops may have formed as a result of the eruption, and not represent a pre-existing loop system heated to soft X-ray temperatures by coronal activity. The newly formed loop system gradually fades over a period of days, without any associated eruption.

In Fig. 9 we illustrate the example of a loop system observed on 29th May 1998 on the solar disk. An increase in the SXT light curve of this region was seen at 09:30 UT, followed by brightening in the lead up to CME onset at 11:43 UT and dimming and disappearance after a second CME at 17:38 UT. This disappearance is illustrated by a lightcurve and shows the lifetime of this TLS to be ≈16 hours. This was one of the shortest lived TLS in our study.

Table 3. Asymmetry of TLS footpoints about the equator, asymmetry of the TLS footpoints in Longitude, and the magnitude of the latitude difference in degrees. The solid line separates Category A TLS (above) from Category B (below).

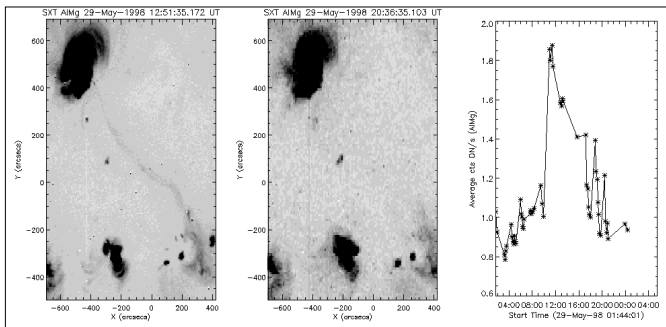| Date	Asymmetry (Latitude)	Asymmetry (Longitude)	Latitude difference	#ARs
10-Sep.-97	3	27	47	2
21-Oct.-97	11	2	29	1
6-May-98	10	37	44	2
27-May-98	6	37	42	2
29-May-98	4	34	48	2
15-Oct.-98	6	17	36	2
04-Nov.-98	7	12	43	2
25-Nov.-98	2	9	36	2
05-Dec.-98	0	32	32	2
12-Mar.-00	7	29	41	2
02-Feb.-96	19	1	21	0
18-Dec.-96	18	14	18	2
31-Jan.-97	3	48	3	1
23-May-97	8	33	12	1
28-Dec.-97	2	40	42	2
13-May-98	5	4	45	1
16-Jun.-98	15	18	49	0
15-Nov.-98	19	1	21	1

Fig. 9. The changing morphology of a TLS observed on 29th May 1998 with north and south locations N26E21 and S22W13 respectively. The first panel shows the brightened TLS following the first CME onset (11:43 UT). The second panel shows the same region following the second CME onset (17:38 UT) and TLS disappearance. The third panel shows the SXT light curve of the TLS showing the decrease in intensity back to background levels following the second CME. SXT data has a resolution of 4.9″.

4. Discussion

The series of homologous eruptions studied by Khan & Hudson (2000) each occurred in association with a flare of magnitude M3.1 or above. Each CME onset considered as part of the present study of 18 TLS was also accompanied by flaring from one or more of the connected active regions.

We found that while the TLS studied by Khan & Hudson (2000) disappeared on three consecutive occasions in association with a flare of M-class or above in each case, the occurrence of an M-class flare does not appear to be a requirement for eruptive interconnecting loops. The series of events from 27–29th May 1998, that resulted in TLS brightening, were connected to active regions both associated with flaring and CME onsets as the system rotated around the west limb. The TLS did not disappear in association with the strongest of the asso-

ciated flares from the connected active regions. In both cases described in Section 3.1, flares associated with CME onset and TLS brightening were C-class, rather than the M and X-class events associated with the eruption of the Khan & Hudson TLS.

The TLS studied by Khan & Hudson (2000), was connected to NOAA AR 8210 in the southern hemisphere. This active region has been the subject of a number of studies owing to its unusually active nature for the period of the solar cycle during which it was observed. Warmuth et al. (2000) describe the evolution of this region in white light and Hα data, which was dominated by a large, rapidly rotating delta spot. Sterling & Moore (2001) also studied this region in terms of its sigmoidal morphology and a series of homologous flares occurring on the 1st and 2nd May 1998, just prior to the appearance of a clear transequatorial connection between active regions.

As mentioned in the introduction, Pevtsov (2000) found 85% of 87 TLS to have footpoints in either hemisphere separated in latitude such that the difference in rotation rate experienced by the two regions would be less than 1°/day. Thus it was assumed that in the majority of cases, differential rotation would not have significant effect on the morphology of the TLS.

In order to confirm this result for the present cases and determine whether a connection might exist between a difference in rotation rate of the two TLS footpoints and the TLS probability of eruption, it was decided to calculate the deviation from symmetry about the equator of those TLS found to be associated with CME onset.

The latitudinal asymmetry of the footpoints of a transequatorial loop was found by calculating the difference in latitude in each hemisphere of the footpoints. In addition, the longitudinal asymmetry was found by taking the difference in longitude. The latitudinal extent, used here to give a measure of TLS length, was then determined by summing the latitudinal position of each footpoint. Table 3 illustrates these results. Using

these values to determine the difference in rotation rate at each end of the TLS gives a maximum difference of only 0.3°/day. Thus, a gradual buildup of shear over a number of days would be required if differential rotation were the cause of TLS eruption. If it is assumed that the loops form as they appear in soft X-ray data, the action of differential rotation would be insufficient to cause strong shearing within the TLS. On average, the events that are not related to a CME have a mean latitudinal asymmetry of 11.1°, a longitudinal asymmetry of 19.8°, and a latitude difference of 26.4°. However, for those events that are associated with CMEs, the mean latitudinal asymmetry is lower at 5.1°, and both the longitudinal asymmetry and the latitude difference (length) are, on average, larger with an average of 23.6° and 39.8° respectively. This suggests that the asymmetry in latitude is not important for the eruption of a TLS. It is more important for the TLS to be extended (no TLS associated with CMEs had a latitude difference less than 29°) and to have a large longitudinal asymmetry.

5. Conclusions

This study provides the first survey of transequatorial interconnecting loops in terms of their eruptive characteristics. These eruptions have been shown to lead to a variety of different signatures. These signatures include the formation of bright soft X-ray cusp shaped features interconnecting active regions, with temperatures equivalent to those observed in active regions during B-class flaring. In addition, there are occasions where dimming of the loop is observed and the more striking homologous disappearances observed by Khan & Hudson (2000). There are also events where the loop appears to remain unchanged by the eruption but the eruption clearly originates from one of the connecting active regions. Taking into consideration that the region studied by Khan & Hudson was one of unusual complexity and high activity, this present study illustrates that transequatorial loops may possess eruptive character, although this is certainly not true of every example. Eruption may also be associated with only moderate levels of flaring (e.g. C-class level). A flare of magnitude greater than M-class is not necessary for a TLS to show eruptive characteristics. It is more common for a TLS to show a response to a CME, and hence provide mass to the CME, if one or more of the following criteria are met;

(a) two active regions are involved;
(b) the TLS is extended, or;
(c) the longitudinal asymmetry is high.

This study considers a relatively small sample of transequatorial loop systems. A larger sample may provide further examples of interconnecting soft X-ray brightenings formed as a result of CME onset. This may also help to address the question of whether projection effects influence the observation of eruptive features in TLS. It should be noted that all interconnecting "cusp" observations made during this study occurred when the relevant system was approaching the west limb, as shown in Table 1. An extended study may also provide further

information as to whether the shear induced by longitudinal asymmetry leads to destabilisation of the loop systems. The advent of 2-D measurements available following the launch of the STEREO mission will undoubtedly lead to further progress in understanding the nature of these features.

References

Andrews, M. D., & Howard, R. A. 1999, in Solar Wind 9, ed. S. R. Habbal, R. Esser, J. V. Hollweg, & P. A. Isenberg, AIP Conf. Proc., 471, 629
Babcock, H. W. 1961, ApJ, 133, 572
Brueckner, G. E., Howard, R. A., Koomen, M. J., et al. 1995, Sol. Phys., 162, 357
Canfield, R. C., Hudson, H. S., & McKEnzie, D. E. 1999, Geophys. Res. Lett., 26, 6, 627
Chase, R. C., Kreiger, A. S., Svestka, Z., & Vaiana, G. S. 1976, in Space Research XVI: Proc. of the Open Meetings of the Working Groups on Physical Sciences and Symposium and Workshop Results from Coordinated Upper Atmosphere Measurement Programmes, 917
Delaboudiniere, J.-P., Artzner, G. E., Brunaud, J., et al. 1995, 162, 291
Domingo, V., Fleck, B., & Poland, A. I. 1995, Sol. Phys., 162, 1
Farnik, F., Karlicky, M., & Svestka, Z. 1999, Sol. Phys., 187, 1, 33
Feldman, U., Laming, J. M., & Doschek, G. A. 1995, ApJ, 451, L79-81
Foley, C. R., Patsourakos, S., Culhane, J. L., & MacKay, D. 2002, A&A, 381, 1049
Glover, A., Ranns, N. D. R., Harra, L. K., & Culhane, J. L. 2000, Geophys. Res. Lett., 27, 13, 2161
Harrison, R. A. 1986, A&A, 162, 1-2, 283
Hudson, H. S., & Cliver, E. W. 2001, JGR, 106, A11, 25199
Howard, R. A., Sheeley, N. R. JR, Michels, D. J., & Koomen, M. J. 1985, JGR, 90, 8173
Khan, J. I., & Hudson, H. S. 2000, Geophys. Res. Lett., 27, 8, 1083
Moreno-Insertis, F. 1986, Sol. Phys., 166, 1-2, 291
Pevtsov, A. A. 2000, ApJ, 531, 533
Sheeley, N. R. Jr, Howard, R. A., Koomen, M. J., et al. 1982, SSRv, 33, 219
Sterling, A. S., & Moore, R. L. 2001, JGR, 106, A11, 25227
Svestka, Z., & Howard, R. 1981, Sol. Phys., 71, 349
Thompson, B. J., Plunkett, S. P., Gurman, J. B., et al. 1998, Geophys. Res. Lett., 25, 14, 1465
Thompson, B. J., Gurman, J. B., Neupert, W. M., et al. 1999, ApJ, 517, L151
Tsuneta, S., Acton, L., Bruner, M., et al. 1991, Sol. Phys., 136, 37
Tsuneta, S., Hara, H., Shimizu, T., et al. 1992, Sol. Phys., 44, 5, L63
Tsuneta, S. 1996, ApJ, 456, L63
Wang, T., Yan, Y., Wang, J., Kurokawa, H., & Shibata, K. 2002, ApJ, 572, 1, 580
Warmuth, A., Hanslemeier, A., Messerotti, M., et al. 2000, Sol. Phys., 194, 1, 103